FINITE ELEMENT ANALYSIS USING ANSYS OF THE PHASE CHANGE MATERIAL (PCM) COOLING SYSTEM ON A 3V LIFEPO4 BATTERY CELL FOR BATTERY PACK APPLICATION

Teyzar Shafatullah[1)*], Baiti Hidayati[1)], Mohd A.F Rosli[2)]
[1)]Department of Mechanical Engineering, Politeknik Negeri Sriwijaya
Jl. Srijaya Negara, Bukit Besar, Kota Palembang, Indonesia
[2)]Management and Science University
University Drive, Off Persiaran Olahraga, Section 13, 40100 Shah Alam, Selangor Darul Ehsan, Malaysia
[*] Corresponding email: baiti.hidayati@polsri.ac.id

ARTICLE INFORMATION

Revised
07/04/2026

Accepted
04/05/2026

Online Publication
11/05/2026

©2026 The Authors. Published by AUSTENIT (Indexed in SINTA)

doi:

10.36257/austenit.v18i1.11876

ABSTRACT

Passive thermal management in $LiFePO_4$ cells was evaluated using three Phase Change Material (PCM) formulations through transient thermal analysis in ANSYS Workbench at charging rates of 1 C, 2 C, and 3 C. The PCM tested consisted of PCM1 (90 wt% paraffin + 10 wt% expanded graphite), PCM2 (n-docosane), and PCM3 (Suntech P116 paraffin wax). At a speed of 1 C, PCM1 produced the most even temperature distribution with a range of only 26.03–27.45 °C (ΔT ≈ 1.42 °C), PCM2 showed a peak temperature of 27.50 °C, while PCM3 succeeded in suppressing the peak temperature to the lowest value of 27.04 °C. At a speed of 2 C, PCM1 maintained an even temperature distribution in the range of 39.67–54.73 °C (ΔT ≈ 15.1 °C), PCM2 recorded the highest peak temperature of 56.28 °C, and PCM3 reached the lowest peak temperature of 53.54 °C. At a discharge rate of 3 C, PCM1 minimizes the temperature gradient with the same range of 39.67–54.73 °C (ΔT ≈ 15.1 °C), PCM2 acts as a heat buffer with a peak temperature of 56.28 °C, while PCM3 remains the most effective in suppressing the peak temperature to 53.54 °C. Overall, PCM1 excels in maintaining the uniformity of temperature distribution, while PCM3 consistently produces the lowest peak temperatures across all tested charging rates, making it the strongest candidate for fast charging applications in $LiFePO_4$ cells.

Keywords *: $LiFePO_4$, Phase Change Material, Paraffin, Thermal Management*

1 INTRODUCTION

ANSYS is designed for conducting engineering analyses in structural and heat transfer fields, employing finite element methods (Kohnke, 1982). Finite element analysis uses numerical methods to estimate solutions while accurately representing the complexities of the problem, including different shapes, boundary conditions, and loads. Flexibility and versatility have sparked considerable interest in engineering (S. S. Bhavikatti, 2005).

Due to the utilization of high-density phase change material (PCM) that provides excellent energy efficiency and needs very little upkeep, passive thermal management has garnered significant attention (Lin et al., 2015). Storing thermal energy is crucial for increasing energy efficiency in various primary thermal energy sources, each with its unique circumstances (Alva et al., 2018). Thermal energy storage (TES) systems provide both environmental and economic benefits by reducing the reliance on burning fuels. Thermal energy storage systems are created to avoid the waste of thermal energy by storing extra heat until it is needed. Heat is produced in almost all human activities, and together, our actions in places like the kitchen and automotive result in a significant amount of heat that is continuously lost. This offers opportunities for new, cost-effective ways to use waste heat (Alva et al., 2018).

Thermal cooling systems, utilized in air conditioning and refrigeration for a long time, utilize various thermodynamic cycles and technologies to meet different capacities. However, their use has been limited because they are less efficient and more expensive initially than traditional mechanical vapor compression systems. Cooling systems are categorized as free cooling systems, air-conditioning systems with PCM, PCM cooling systems with absorption and adsorption, and encapsulated PCM systems/heat exchangers.

Inside these groupings, studies were separated depending on whether they were conducted through experimentation or simulation (Osterman et al., 2012).

Swift growth of the lithium-ion battery sector has impacted how individuals consume and live their lives. LiFePO4 (LFP) batteries, which are a major kind of Lithium-ion batteries are commonly used in electric cars and storage devices due to their excellent safety and reliable charging abilities (Xu et al., 2024). The battery pack shows the remaining cell capacity, while absorbable capacity is the lowest chargeable capacity. The total pack capacity is comprised of the remaining cell capacity plus the minimum chargeable capacity (Cicconi & Kumar, 2023).

The objective of this study is to design a Phase Change Material (PCM) based cooling system for a 3.2 V LiFePO4 battery using SolidWorks and to evaluate the thermal management performance of the same type of PCM in cooling the battery at discharge rates of 1C, 2C, and 3C through simulation and analysis using ANSYS Workbench.

2. MATERIALS AND METHODS

2.1 Material Description

The use of FEA analysis, specifically the finite element method (FEM) using ANSYS software by using the transient thermal analysis available in Ansys software (Kohnke, 1982). This study will focus on using paraffins because pure paraffin wax and commercial grade paraffin wax have good thermal stability and retain their properties after 1000 to 2000 cycles (Pielichowska & Pielichowski, 2014), according to the literature. paraffin wax does not corrode, it is safe, does not react with other materials, and can be used in metal containers (Farid et al., 2004; Fernandes et al., 2012) . With the help of Solidworks, a phase change material (PCM) based cooling system for 3.2V LiFePo4 battery has been designed. ANSYS Workbench to evaluate the thermal management performance of same PCM types in cooling the battery under 1C, 2C and 3C discharge rates through simulation and analysis using Ansys.

PCM thermophysical properties include latent heat, phase-change temperatures, enthalpy, and specific heat capacity. These features help characterize PCMs for thermal energy storage technologies to improve latent heat storage system design. Table 1 will explain the thermophysical properties of the materials that will be used for the Phase Change Material (PCM) based cooling system.

Table 1. Engineering Data Sources

Property	PCM 1	PCM 2	PCM 3
	90 wt% paraffin/10 wt% EG	n-docosane	Suntech P116 Paraffin Wax
Density (kg/m^3)	721	785	818
Melting Temperature (K)	313.35	313.35	316
Isotropic Thermal Conductivity (W/m·K)	0.820	0.220	0.524
Specific Heat Constant Pressure (J/kg·K)	2380	2380	2950
Entalphy (J/m^3)	12875830	15216100	21758800

(Sari & Karaipekli, 2007; Himran et al., 1994)

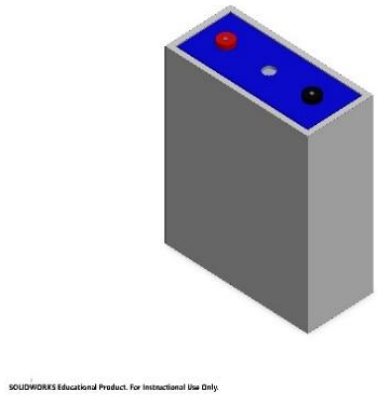

Figure 1. 3.2V LiFePo4 Battery with PCM

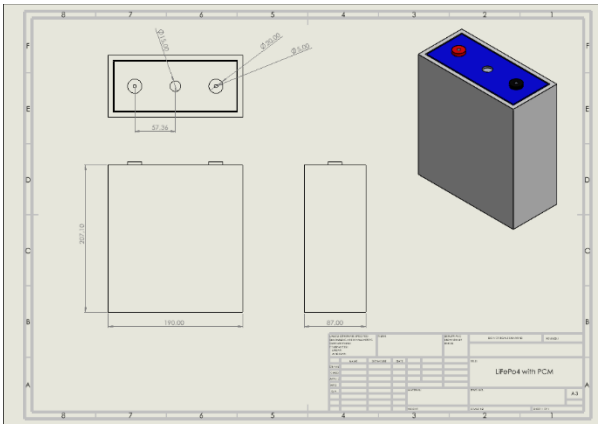

Figure 2. Technical Drawing LiFePo4 with PCM

The function of the phase change material is to control the temperature rise due to thermal cycling. Figure 1 shows a picture of a battery that has been installed with a phase-change material cooling system.

Table 2 will explain the specifications of LiFePO4 battery from Shenzhen Xiho Energy Technology Co., Ltd. company to calculate the heat generation with 1C, 2C and 3C discharge rate for the needs of table 3 parameters in transient thermal analysis. To calculate the heat generation in the battery we need information on the rated capacity, internal resistance, dimensions of the LiFePO4 battery by Eq. (1-5):

$$I = Rated\ Capacity\ (Ah)\ \times\ C - rate \quad (1)$$

$$R(\Omega) = \mathrm{R(m\Omega)} \times 10^{-3} \quad (2)$$

$$Q = I^2 \times R \quad (3)$$

$$V = Length \times Widht \times Height \quad (4)$$

$$q''' = \frac{Q}{V} \quad (5)$$

This battery is expected to generate about 6044.41 W/m³, 24716.78 W/m3 and 54401.09 W/m3 of heat at a discharge rate of 1C, 2C and 3C. This number indicates how much heat is generated per unit volume as a result of internal resistance when Sthe battery is continuously discharged at its maximum rate

Table 2. LiFePO4 Battery Parameters

Product Parameters	Value
Nominal Voltage (V)	3.2
Internal Resistance (mΩ)	≤ 0.2
Cycle Life (times)	> 1000
Weight (Kg)	5.43 ± 0.3
Rated Capacity (Ah)	280
Max Charge Voltage (V)	3.65
Max Discharge Rate (C)	1
Discharging Temperature (℃)	15 ~ 60
Dimension (mm)	71.7*174.7*207.1

Table 3. LiFePO4 Battery Thermal Parameters

Parameters	LiFePO4
Density (kg/m^3)	2118
Isotropic thermal Conductivity (W/m·K)	15.12
Specific Heat Constant Pressure (J/kg·K)	1029.49
Heat Generation 1C	6055.98
Heat Generation 2C	24716.78
Heat Generation 3C	54401.09

(Song et al., 2023)

Table 4. Thermal Load Parameters

Name	Parameters
Convection (W/$m^2 \cdot C$)	12,5
Ambient Temperature (℃)	25

2.2 Model Setup

Good quality finite element mesh was generated to ensure accurate thermal analysis results for both configurations: the battery alone and the battery encapsulated with PCM. Separate meshing strategies were employed for the battery and PCM components based on their geometric complexity.

Mesh convergence study was conducted to verify the stability and accuracy of temperature predictions prior to analysis. The study involved varying the mesh size and monitoring the change in maximum battery temperature under identical boundary conditions. The goal was to ensure that the solution becomes independent of mesh refinement beyond a certain threshold. The convergence results for PCM 1 are summarized in table 5.

Table 5. Mesh convergence against maximum temperature using PCM 1

Mesh Size (mm)	Max Battery Temperature (°C)	Percentage Error (%)
12	22.260	-
11	23.980	7.72
10	24.560	2.41
9.0	25.820	5.13
8.0	26.224	1.56
7.0	26.276	0.19

Based on mesh convergence above a mesh size of 8 mm was chosen for analysis purposes because it gives error less than 5%.

The PCM domain was meshed using quadratic hexahedral elements (second-order brick elements), which are known for their high accuracy in capturing thermal gradients in structured geometries. A uniform mesh size of 8 mm was used throughout the PCM volume to maintain consistency across all PCM materials as shown in Figure 3.

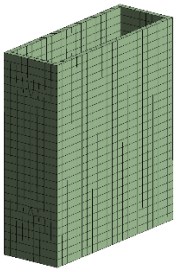

Figure 3. Meshing of PCM

Due to the presence of complex geometry and curvature in the battery model, tetrahedral elements were employed for meshing. These elements offer greater flexibility in fitting to irregular geometries. A mesh size of 8 mm was also used here to maintain compatibility and reduce computational time as shown in figure 4.



Figure 4. Meshing of Battery

The final mesh used in the simulation consisted of total nodes 59,855 and total elements

34,053. This mesh provided a good balance between computational efficiency and accuracy for transient thermal analysis of both the battery and PCM domains.

A perfect thermal contact was assumed at the battery PCM interface to ensure efficient thermal conduction for this reason bonded connection of ANSYS was utilized as shown in figure 5.

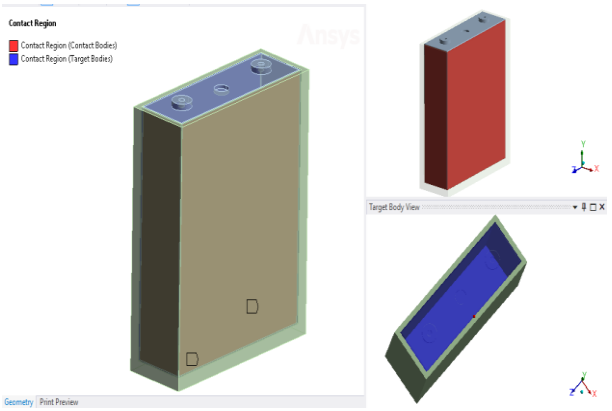

Figure 5. Thermal Contact Between Battery and PCM Casing

2.3 Analysis Setup

Transient thermal analysis was performed to investigate the temperature distribution and heat flux in a lithium-ion battery during operation (Hendra et al., 2025). The use of transient analysis is critical due to the time-dependent nature of thermal behavior in batteries, which cannot be accurately captured using steady-state assumptions. The simulation was run for a total duration of 3500 seconds, based on operational time and methodology from the reference study.

The analysis was carried out under three primary load cases to simulate different charging/discharging rates, 1C Heat Generation Rate (6055.98 W/m3), 2C Heat Generation Rate (24716.78 W/m3), 3C Heat Generation Rate (54401.09 W/m3) Each load case was analyzed under two physical configurations: Battery alone configuration (without PCM) and Battery with PCM enclosure configuration

In the first configuration, the battery was modeled without any surrounding Phase Change Material (PCM). The entire battery domain was initialized at 25°C, and two levels of internal heat generation were applied to simulate different operational intensities: 1C, 2C and 3C discharge rates (Fahlovi et al., 2025). The corresponding volumetric heat generation values were applied directly to the battery geometry. In addition to internal heating, natural convection was applied to all outer surfaces of the battery using a convective heat transfer coefficient of 12,5 W/m²·K, with the surrounding environment maintained at 25°C. This setup allows for heat dissipation from the battery to the ambient environment via convection. Thermal flux through the surfaces was also considered to account for surface heat transfer effects. The three load cases 1C, 2C and 3C were simulated separately to assess the thermal response under normal and accelerated discharge rates. The overall boundary conditions used for analysis are shown in figure 6 (a) (b) (c).

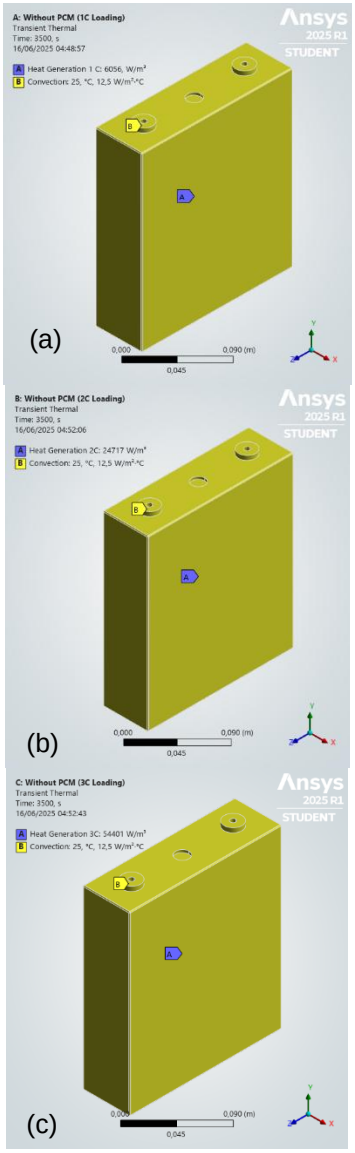

Figure 6. (a) 1C Boundary Condition for Battery Alone, (b) 2C Boundary Condition for Battery Alone, and (c) 3C Boundary Condition for Battery Alone

In the Second configuration, the battery was enclosed with a layer of PCM to assess the effect of passive thermal management. The initial temperature for both the battery and the surrounding PCM was set to 25°C. The same internal heat generation values corresponding to 1C, 2C, and 3C rates were applied to the battery, while no internal heat generation was assigned to the PCM. While heat flux and natural convection

was applied to the outer surface of the PCM layer. The overall boundary conditions used for analysis are shown in figure 7 (a) (b) (c).

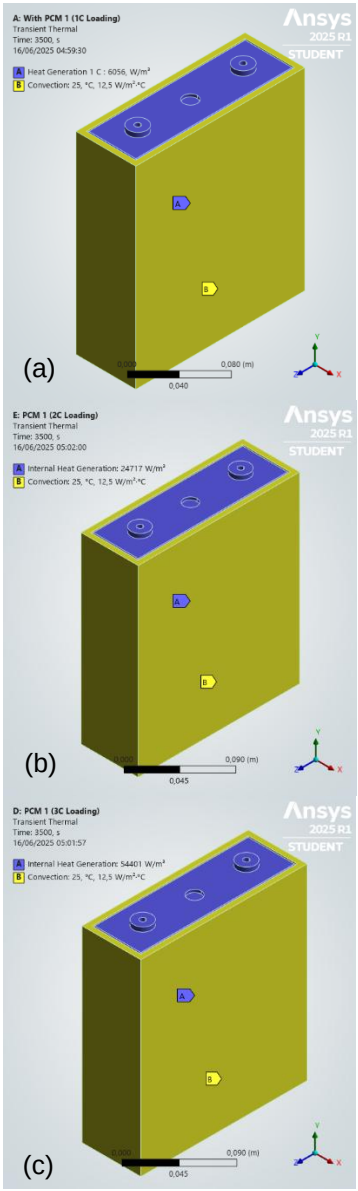

Figure 7. (a) 1C Boundary Condition for Battery with PCM, (b) 2C Boundary Condition for Battery with PCM, and (c) 3C Boundary Condition for Battery with PCM

3. RESULTS AND DISCUSSION

The thermal performance of the lithium-ion battery under three different load cases 1C, 2C and 3C heat generation was evaluated using transient thermal analysis. Both configurations, battery alone and battery with PCM, were analyzed to assess the temperature distribution and heat flux behavior over a 3500 second operational period.

3.1 Temperature Distribution for 1C Load

Figure 8 provides a comparison between the four conditions of 1 C shows that without PCM, the $LiFePO_4$ cell reaches a maximum temperature of 29.70 °C, an average of 29.57 °C, and a minimum of 29.33 °C after 3,500 seconds. The highest temperature drops to 27.45 °C with PCM1 (90 wt% paraffin + 10 wt% EG), the average temperature drops to 27.18 °C, and the lowest temperature drops to 26.03 °C. This means that the highest temperature drops by about 2.25 °C and the lowest temperature drops by 3.30 °C. PCM2 (n-docosane) had a similar effect, with a peak of 27.50 °C, an average of 27.17 °C, and a minimum of 25.24 °C. The minimum temperature drop was about 4.10 °C.

The most effective PCM3 (Suntech P116 paraffin wax) brought the peak down to only 27.04°C, the average down to 26.69°C, and the minimum down to 24.96°C. These differences of ~2.66°C, ~2.88°C, and ~4.38°C are the biggest compared to the case without PCM. The order of thermal management effectiveness is PCM3 (Suntech P116 paraffin wax) > PCM2 (n-docosane) > PCM1 (90% paraffin and 10% EG). This means that Suntech Paraffin Wax has the best ability to absorb latent heat and smooth out temperature peaks to keep thermal stability and extend cell cycle life at 1 C continuous load.

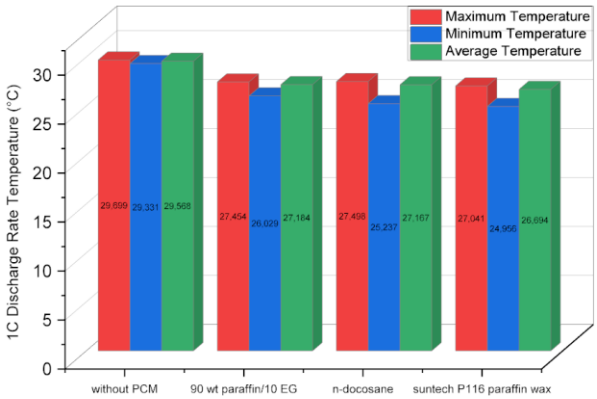

Figure 8. Battery Temperature 1C Load

3.2 Temperature Distribution for 2C Load

The comparison in Figure 9 at a constant load of 2 C for 3,500 s shows that the $LiFePO_4$ cell gets very hot without PCM, reaching a maximum temperature of 47.30 °C, an average of 46.67 °C, and a minimum of 45.53 °C. Adding PCM1 (90% paraffin and 10% EG) lowers the peak temperature to 37.98 °C (about 9.3 °C lower), the average temperature to 36.80 °C, and the minimum temperature to 31.30 °C. This shows that some latent heat has been activated. PCM2 (n-docosane) only worked well because it didn't reach its melting point of about 44 °C. It worked best at 38.61 °C and averaged 37.15 °C, but it lowered the minimum

temperature even more to 27.36 °C because of its specific heat capacity.

PCM3 (Suntech P116 paraffin wax) worked the best, lowering the peak temperature to 37.27 °C, the average to 35.79 °C, and the minimum to 26.78 °C. This made the maximum-minimum thermal gradient about 10.49 °C. All three PCMs were able to keep the temperature from rising compared to not using any PCMs. PCM3 was the best at cooling across all three-temperature metrics, making it the best choice for high-load battery cooling applications during these simulations.

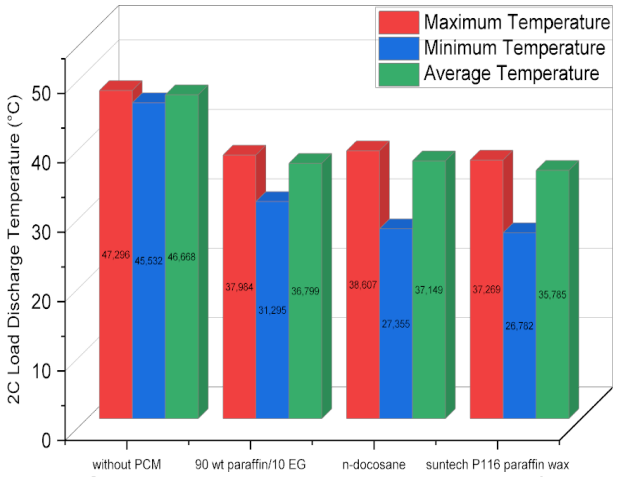

Figure 9. Battery Temperature 2C Load

3.3 Temperature Distribution for 3C Load

Figure 10 provides a comparison between the four conditions of 3 C shows that without PCM, the $LiFePO_4$ cell reaches a maximum temperature of 75.29 °C, an average of 71.3 °C, and a minimum of 73,87 °C after 3,500 seconds. The highest temperature for PCM 1 (90% paraffin + 10% EG) is about 54.73 °C, the lowest is about 39.67 °C, and the average is about 52.09 °C. The temperature range is about 15.1 °C. This shows that the temperature distribution is the most even, even though it is still in the middle. PCM 2 (n-docosane) kept the temperature from rising for a longer time; the highest value was only about 56.28 °C and the lowest value was about 30.72 °C. The range was wider, though, at about 25.6 °C.

This means that latent heat worked, but heat absorption wasn't even. PCM 3 (Suntech P116 paraffin wax) had the best peak temperature drop (about 53.54 °C) and the lowest average temperature (about 50.25 °C). It also had the lowest minimum temperature, which was about 29.65 °C, and a range of about 23.9 °C. This made it the best at keeping cells from getting too hot. PCM 3 (Suntech P116 paraffin wax) did the best job of keeping the highest and lowest temperatures low, while PCM 1 (90% paraffin and 10% EG) did the best job of keeping the temperature difference between the cells low.

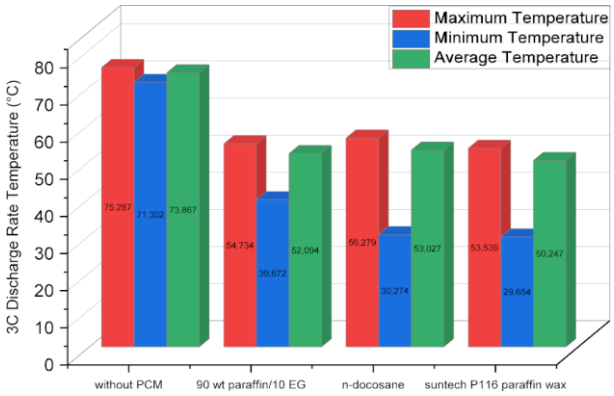

Figure 10. Battery Temperature 3C Load

4. CONCLUSION

This study shows that integrating PCM into $LiFePO_4$ cell packages consistently improves thermal management through peak temperature reduction, temperature gradient flattening, and increased total heat flux to the PCM medium. At a charging rate of 1 C load, without PCM, the cell reaches a peak temperature of 29,70 °C with a local gradient of only ≈0,37 °C, while with PCM3 (Paraffin P116), the peak temperature dropped to 27,04 °C ($\Delta T \approx 2.66$ °C). At a rate of 2 C load, PCM3 reduces the peak temperature from 47,30 °C to 37,27 °C ($\Delta T \approx 10.03$ °C), confirming the efficiency of PCM in controlling the melting phase and slowing the rise in cell core temperature. At a 3 C load, PCM1 (Paraffin + EG) also lowered the peak temperature from 75,29 °C to 54,73 °C ($\Delta T \approx 20,56$ °C) with a temperature range of ≈15,1 °C. This shows that PCM is an effective thermal buffer that can withstand and spread heat under extreme load conditions. PCM can absorb both sensible and latent heat and control the flow of total heat flux. This has been shown to extend the life of cells, improve thermal stability, and lower the risk of hot spots in different operating conditions.

REFERENCES

Alva, G., Lin, Y., & Fang, G. (2018). An overview of thermal energy storage systems. *Energy*, *144*, 341–378. https://doi.org/10.1016/j.energy.2017.12.037

Cicconi, P., & Kumar, P. (2023). Design approaches for Li-ion battery packs: A review. *Journal of Energy Storage*, *73*, 109197. https://doi.org/10.1016/j.est.2023.109197

Fahlovi, O., Ramadhan, S., & Setyawan, H. (2025). Analisis Getaran Dan Ketidaksejajaran Pada Pompa Sentrifugal: Identifikasi Kerusakan Pada Rubber Coupling. *AUSTENIT*, *17*(1), 1–9. https://doi.org/10.53893/austenit.v17i1.10629

Farid, M. M., Khudhair, A. M., Razack, S. A. K., & Al-Hallaj, S. (2004). A review on phase change energy storage: materials and applications. *Energy Conversion and Management*, *45*(9–10), 1597–1615. https://doi.org/10.1016/j.enconman.2003.09.015

Fernandes, D., Pitié, F., Cáceres, G., & Baeyens, J. (2012). Thermal energy storage: "How previous findings determine current research priorities." *Energy*, *39*(1), 246–257. https://doi.org/10.1016/j.energy.2012.01.024

Hendra, Abdulah, B., Ula, S., Septiana, R., Hernadewita, & Hermiyetti. (2025). Pengaruh Paduan Jenis Plastik Pp, Hdpe, dan Ldpe Daur Ulang Terhadap Sifat Mekanik Balok Plastik Hasil Inejction Molding. *AUSTENIT*, *17*(1), 10–16. https://doi.org/10.53893/austenit.v17i1.10589

Himran, S., Suwono, A., & Mansoori, G. A. (1994). Characterization of alkanes and paraffin waxes for application as phase change energy storage medium. *Energy Sources*, *16*(1), 117–128. https://doi.org/10.1080/00908319408909065

Kohnke, P. C. (1982). ANSYS. In *Finite Element Systems* (pp. 19–25). Springer Berlin Heidelberg. https://doi.org/10.1007/978-3-662-07229-5_2

Lin, C., Xu, S., Chang, G., & Liu, J. (2015). Experiment and simulation of a LiFePO4 battery pack with a passive thermal management system using composite phase change material and graphite sheets. *Journal of Power Sources*, *275*, 742–749. https://doi.org/10.1016/j.jpowsour.2014.11.068

Osterman, E., Tyagi, V. V., Butala, V., Rahim, N. A., & Stritih, U. (2012). Review of PCM based cooling technologies for buildings. *Energy and Buildings*, *49*, 37–49. https://doi.org/10.1016/j.enbuild.2012.03.022

Pielichowska, K., & Pielichowski, K. (2014). Phase change materials for thermal energy storage. In *Progress in Materials Science* (Vol. 65, pp. 67–123). Elsevier Ltd. https://doi.org/10.1016/j.pmatsci.2014.03.005

S. S. Bhavikatti. (2005). *Finite Element Analysis: 334 halaman*. New Age International.

Sari, A., & Karaipekli, A. (2007). Thermal conductivity and latent heat thermal energy storage characteristics of paraffin/expanded graphite composite as phase change material. *Applied Thermal Engineering*, *27*(8–9), 1271–1277. https://doi.org/10.1016/j.applthermaleng.2006.11.004

Sarı, A., & Karaipekli, A. (2007). Thermal conductivity and latent heat thermal energy storage characteristics of paraffin/expanded graphite composite as phase change material. *Applied Thermal Engineering*, *27*(8–9), 1271–1277. https://doi.org/10.1016/j.applthermaleng.2006.11.004

Song, L., Huang, Z., Mei, W., Jia, Z., Yu, Y., Wang, Q., & Jin, K. (2023). Thermal runaway propagation behavior and energy flow distribution analysis of 280 Ah LiFePO4 battery. *Process Safety and Environmental Protection*, *170*, 1066–1078. https://doi.org/10.1016/j.psep.2022.12.082

Xu, Y., Zhang, B., Ge, Z., Zhang, S., Song, B., Tian, Y., Deng, W., Zou, G., Hou, H., & Ji, X. (2024). Advances and perspectives towards spent LiFePO4 battery recycling. *Journal of Cleaner Production*, *434*, 140077. https://doi.org/10.1016/j.jclepro.2023.140077